

INVESTIGATION OF MULTI-SCALE ION TEMPERATURE GRADIENT INSTABILITIES IN ADITYA-U TOKAMAK

Amit K. Singh^{1,3,a}, J. Mahapatra^{2,3}, Jugal Chowdhury^{4,*}, R. Ganesh^{2,3}, W.X. Wang⁵, L. Villard⁶, S. Ethier⁵

PAPER ID - 1295

^aEmail: amitks@ipr.res.in¹ITER-India, Institute for Plasma Research, Bhat, Gandhinagar-382428, India²Institute for Plasma Research, Bhat, Gandhinagar-382428, India³Homi Bhabha National Institute, Anushaktinagar, Mumbai-400094, India⁴CFSA, University of Warwick, Coventry, CV47AL, UK⁵Princeton Plasma Physics Laboratory, Princeton 08540, USA⁶Swiss Plasma Center, EPFL, 1015, Lausanne, Switzerland

*Present Address: Sikkim University, Sikkim, India

Abstract

- The ADITYA-U tokamak is a small size tokamak that recently upgraded to divertor configuration and is suitable for studies of micro- instabilities in the presence of steep gradients.
- Global linear and nonlinear simulation studies of the conventional and short scale ion temperature gradient mode (SWITG) for experimental profiles and parameters of ADITYA-U tokamak are carried out.
- Global gyrokinetic PIC code GTS, linear global gyrokinetic code GLOGYSTO and the flux-tube version of GENE are used in simulation study.
- GTS is first benchmarked for ion temperature gradient modes with adiabatic electrons and non-adiabatic ions for the familiar Cyclone DIII-D base case (CBC).
- Good agreement is obtained for the real frequencies and growth rates between different codes for CBC.
- For experimental shot# 29029 of ADITYA-U tokamak, the real frequencies, growth rates and mode structures are calculated using GLOGYSTO and GTS and compared using flux tube GENE code for linear case.
- It is found using linear stability analysis that the SWITGs are suppressed for low values of R/L_n .
- Nonlinear global simulations using GTS for ADITYA-U tokamak are also performed.
- The results for SWITG dominant case are compared with nonlinear runs where SWITG is relatively suppressed.

Introduction

- ❖ The ion temperature gradient mode, which is driven by the temperature gradient of ions is shown to become unstable even at wave lengths $k_\theta \rho_i > 1.0$, in the presence of sharp temperature gradients [1,2].
- ❖ Similarly, trapped electron modes also can manifest a shorter wavelength branch in the presence of strong gradients [3].
- ❖ Such short wavelength branch of micro-instabilities is shown to be crucial for experimental parameters using gyrokinetic simulations [4].
- ❖ Therefore, it is important to understand the nonlinear properties of these multi-scale modes and their contribution to the anomalous transport of particles and energy.
- ❖ Nonlinear flux tube simulation of short wavelength branch of the ion temperature gradient modes considering adiabatic electrons showed that the contribution from the shorter-scale modes to the total heat flux is weaker than the longer wavelength branch [5].
- ❖ However, the region across the steep gradients might be very small and flux tube calculations might not be appropriate under these conditions.
- ❖ But such an assumption fails in the narrow gradient regions. This naturally calls for the necessity of global calculations that treat small scale fluctuations and large scale equilibrium variations on the same footing or in other words a multi-scale study.
- ❖ It is therefore important to investigate how this mode behaves nonlinearly and if there is any significant contribution of this mode to the net ion transport in the core of the system.
- ❖ To this end, we carry out a systematic linear and nonlinear study of the mode for ADITYA-U [6] using global gyrokinetic PIC code GTS [7] and global eigen value gyrokinetic code GLOGYSTO [8].
- ❖ For comparison, in the linear regime, flux tube version of GENE [9,10] is also used.
- ❖ All simulations are done with non-adiabatic ions and adiabatic electrons.

Simulation Model

GTS

- The dynamics of particles in GTS code is determined on the gyrokinetic formalism.
- The time evolution of the perturbed part δf_α of the particle distribution function f_α expressed as the sum of an equilibrium part $f_{\alpha 0}$ and a perturbed part δf_α , where α stands for particle species.
- For the collision less case and electrostatic limit, the gyrokinetic equation for ions ($\alpha = i$), with μ and v_\parallel as independent velocity variables can be written as,

$$\frac{\partial \delta f_i}{\partial t} + (v_\parallel \hat{b} + \vec{v}_{E_0} + \vec{v}_E + \vec{v}_d) \cdot \nabla \delta f_i - \hat{b}^* \cdot \nabla (\mu B + \frac{e}{m_i} \Phi_0 + \frac{e}{m_i} \bar{\phi}) \frac{\partial \delta f_i}{\partial v_\parallel} = -\vec{v}_E \cdot \nabla f_{i0} + \hat{b}^* \cdot \nabla \left(\frac{e}{m_i} \bar{\phi} \right) \frac{\partial f_{i0}}{\partial v_\parallel}$$

Here, \vec{v}_{E_0} and \vec{v}_E are EXB drift velocities resulting, respectively, from the equilibrium potential Φ_0 and turbulent potential $\bar{\phi}$, and \vec{v}_d is the magnetic drift comprising of curvature and ∇B drift velocities \vec{v}_c and $\vec{v}_{\nabla B}$. The definitions are given in the following:

$$\begin{aligned} \vec{v}_{E_0} &= \frac{cb \times \nabla \Phi_0}{B}, \\ \vec{v}_E &= \frac{cb \times \nabla \bar{\phi}}{B}, \\ \hat{b}^* &= \hat{b} + \rho_\parallel b \times (\hat{b} \cdot \nabla \bar{\phi}), \\ \vec{v}_d &= \vec{v}_c + \vec{v}_{\nabla B} = \frac{v_\perp^2}{\Omega_\alpha} \hat{b} \times (\hat{b} \cdot \nabla \bar{\phi}) + \frac{\mu}{\Omega_\alpha} \hat{b} \times \nabla B \end{aligned}$$

With $b = B/B$, $\rho_\parallel = v_\parallel/B$ and $\mu = m_i v_\perp^2/2B$ the magnetic moment. Also, m_α and Ω_α are mass and gyro frequency of species α .

GLOGYSTO

- GLOGYSTO code is a global spectral code.
- Calculates the real frequency and growth rates of unstable modes for a given equilibrium using Nyquist method and also gives the eigen mode structure.
- The perturbed density for a species j , can be expressed as sum of adiabatic and nonadiabatic parts as follows:

$$\tilde{n}_j(\mathbf{r}; \omega) = -\left(\frac{q_j N}{T_j}\right) \left[\tilde{\varphi} + \int d\mathbf{k} \exp(i\mathbf{k} \cdot \mathbf{r}) \int d\mathbf{v} \frac{f_{Mj}}{N} (\omega - \omega_j^*) (iU_j) \tilde{\varphi}(\mathbf{k}; \omega) J_0^2(x_{Lj}) \right]$$

In the above equation q_j and T_j are the charge and temperature for the species j , N stands for the equilibrium density. The diamagnetic drift frequency is given by $\omega_j^* = \omega_{nj} [1 + \frac{\eta_j}{2} (\frac{v_\perp^2}{v_{thj}^2} - 3)]$ where $\omega_{nj} = (T_j \nabla_n \ln k_\theta) / (q_j B)$, $\nabla_n = -r B_\theta \frac{\partial}{\partial \eta}$ and $\eta_j = (d \ln T_j) / (d \ln n)$, v_{thj} is the thermal velocity of species j . The Bessel function $J_0(x_{Lj})$ with $x_{Lj} = k_\perp \rho_{Lj}$, incorporates the full finite Larmor radius effect. Note that here m and n are poloidal and toroidal wave numbers, $q(r)$ is the safety factor, k_θ is poloidal wave vector, B_θ is the poloidal magnetic field. f_{Mj} is a local Maxwellian for species j .

Benchmarking of GTS code

- GTS code is benchmarked for ion temperature gradient modes with a simplified adiabatic response for the electron dynamics for the familiar Cyclone DIII-D base case (CBC) [11].
- INPUT parameters and profiles for CBC:
 - Inverse aspect ratio $a/R_0 = 0.334$, ion temperature profile $R_0/L_T = 6.92 \exp[-(r-r_0)/0.28]6$, $T_e/T_i = 1$, $q = 0.854 + 2.184r^2$, and $\eta = L_n/L_T = 3.145$.
 - Simulation is carried out in a radial domain from 0.1 to 0.9 (in terms of normalized minor radius).
 - The ITG instability is measured at $r_0 = r/a = 0.5$, where the temperature gradient peaks.
 - Six toroidal mode numbers: $n = 5, 10, 15, 20, 25, 30$ which cover the poloidal wave numbers $k_\theta \rho_i$ from 0.1 to 0.7.

Fig. 1

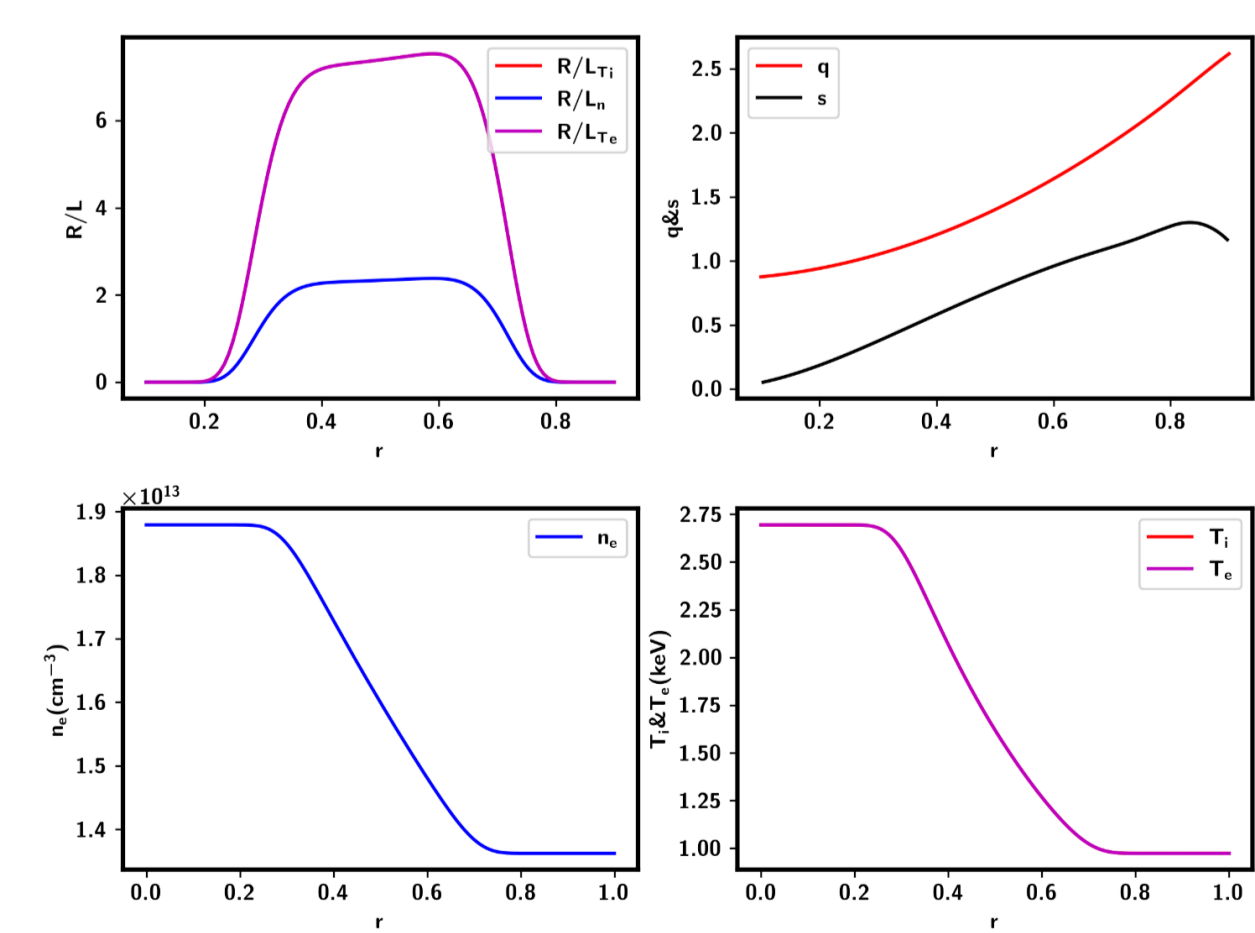


Fig. 3

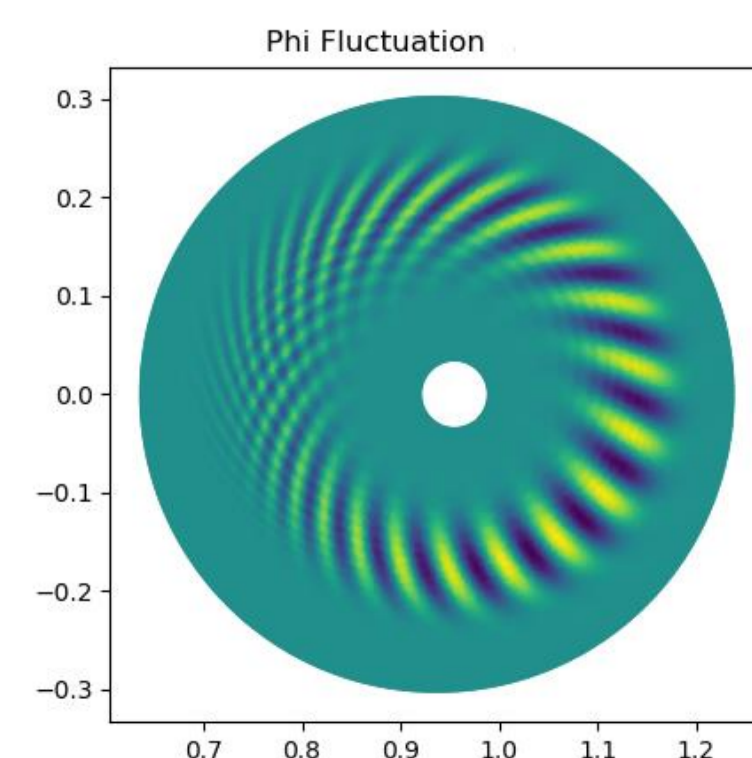
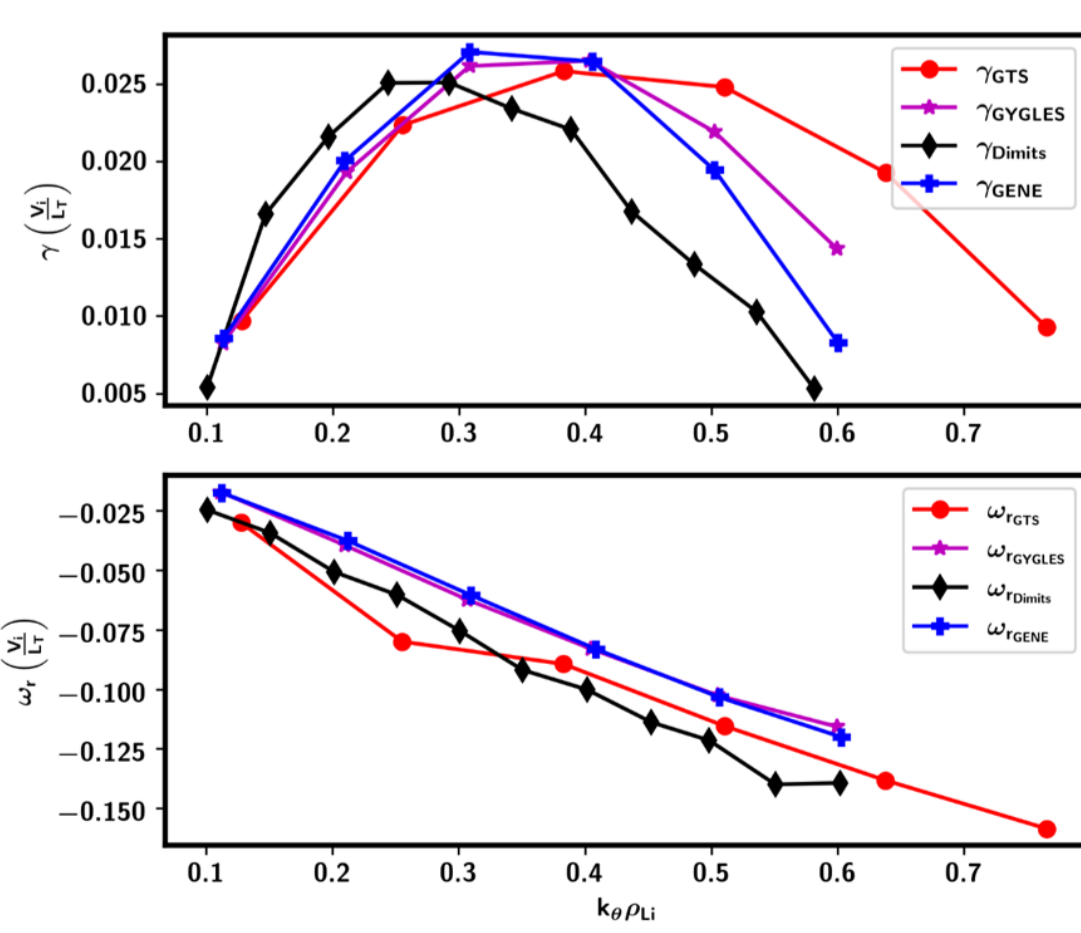


Fig. 2



- Plasma parameters profiles for CBC case are shown in Fig. 1.
- Comparison of growth rate and real frequency of ITG modes between different codes GYGLES, Dimits, GENE, data extracted from published figures and. Note that only GTS results are from present study. The results for other codes are taken from Ref. [10,11] are shown in Fig. 2.
- Mode structure of most unstable mode is shown in Fig. 3.
- Good agreement is obtained for the real frequencies and growth rates between different codes.

Linear simulation of shot# 29029 of ADITYA-U tokamak

- ❖ The ADITYA-U tokamak is a small size tokamak that is recently upgraded to divertor configuration and is suitable for studies of micro- instabilities in the presence of steep gradients.
- ❖ Linear simulations using GLOGYSTO and GTS codes for parameters and profiles of shot# 29029 of ADITYA-U tokamak are carried out for hydrogen plasma in the electrostatic limit.
- ❖ The profiles and parameters that are used in simulation of ADITYA-U are given in below table.

Parameters:

B-field: $B_0 = 1.0$ TeslaTemperature: $T_0 = T(r_0) = 70.5$ eVDensity: $N_0 = N(r_0) = 9.05 \times 10^{12} \text{ cm}^{-3}$ Major Radius: $R = 0.75$ mMinor Radius: $a = 0.25$ mradius: $r = \rho/a$, $r_0 = 0.6$ $L_{n0} = 0.075$ m, $L_{T0} = 0.03$ m $\eta_{ie}(r_0) = L_{n0}/L_{T0} = 2.5$, $\tau = T_e(r)/T_i(r) = 1$ $\epsilon_n = L_{n0}/R = 0.1$, $\epsilon_T = L_{T0}/R = 0.04$

Equilibrium profiles:

N-profile and T-profile:

$$N(r)/N_0 = \exp\left(-\frac{a\delta s_r}{L_{n0}} \tanh\left(\frac{r-r_0}{\delta s_r}\right)\right)$$

$$T_{ie}(r)/T_0 = \exp\left(-\frac{a\delta s_T}{L_{T0}} \tanh\left(\frac{r-r_0}{\delta s_T}\right)\right)$$

$$\delta s_n = 0.35, \delta s_T = 0.2 \text{ at } r = r_0$$

$$q(r) = 1.25 + 0.67r^2 + 2.38r^3 - 0.06r^4$$

$$\text{such that } q(r=r_0) = 2.0;$$

$$\text{Magnetic shear } s \text{ is positive and at } r = r_0, s = 1.0$$

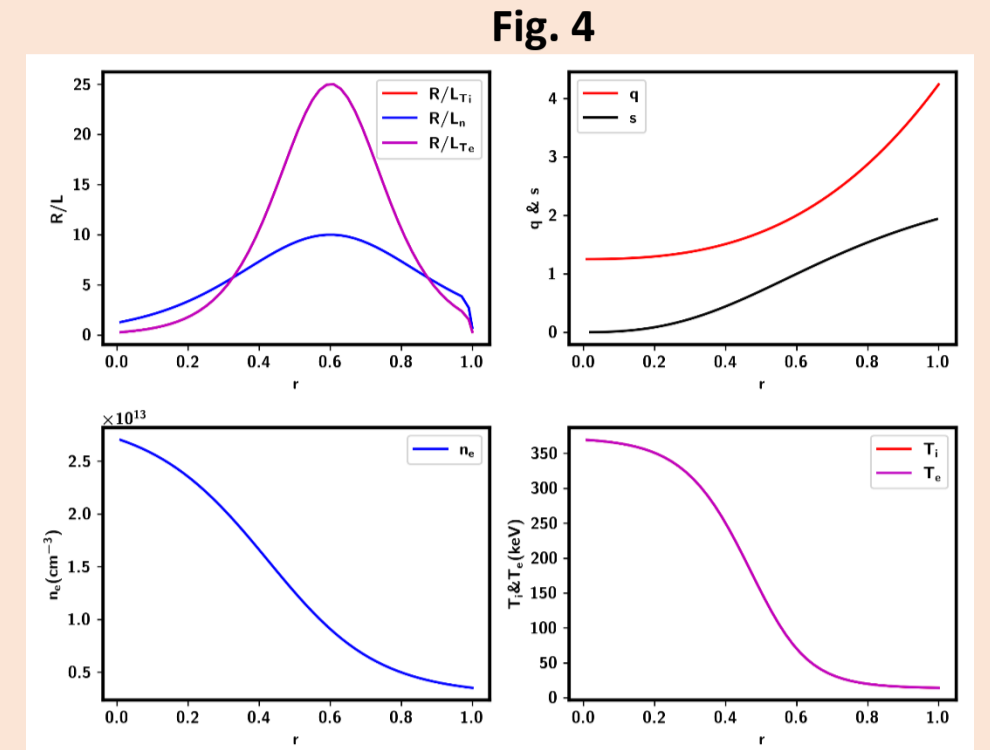


Fig. 4

- ❖ The density, temperature, safety factor and shear profiles for ADITYA-U circular plasma at Z = 0 midplane are as shown in Fig. 4.
- ❖ For the parameters and equilibrium profiles as given in table 1, the growth rates and real frequencies are calculated using GLOGYSTO and GTS for ADITYA-U's $R/L_n = 10$ for different toroidal mode numbers.

Fig. 5

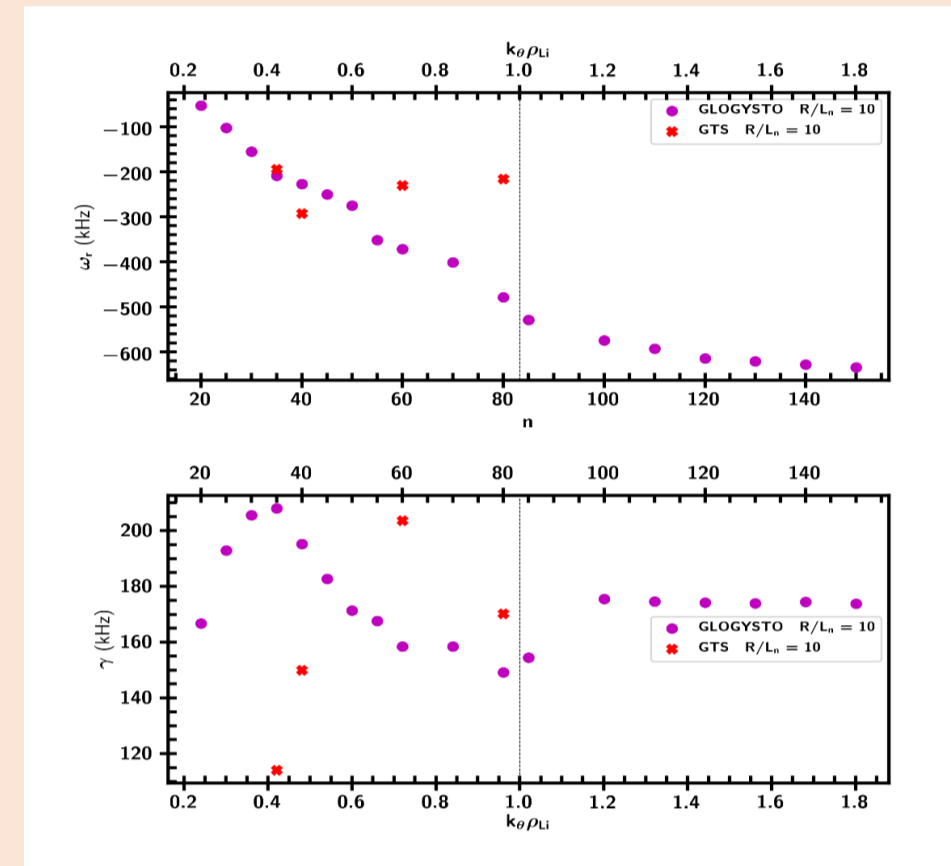


Fig. 6

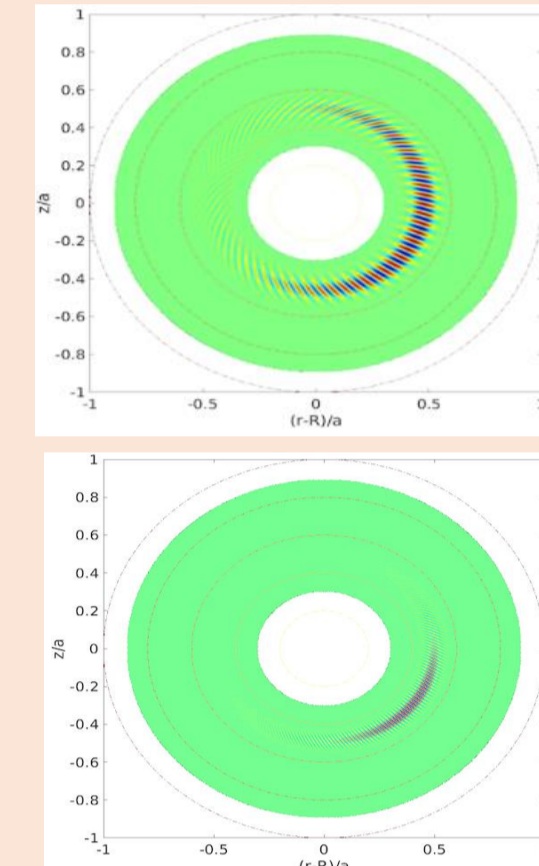
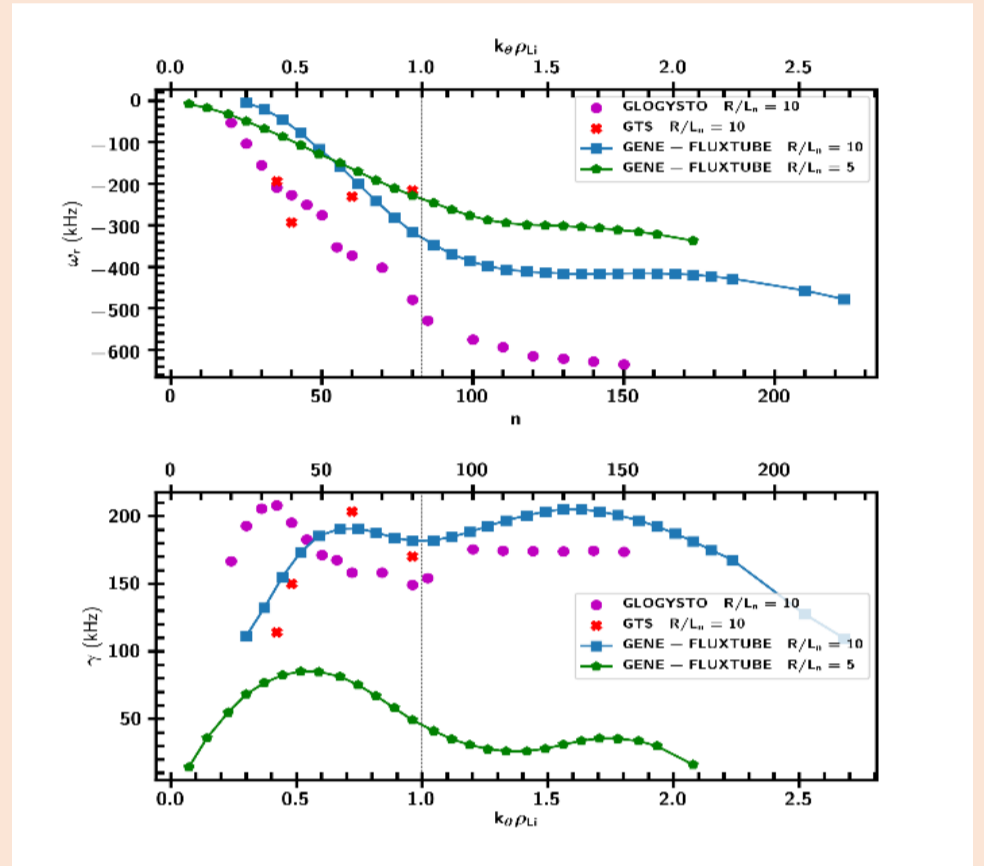


Fig. 7

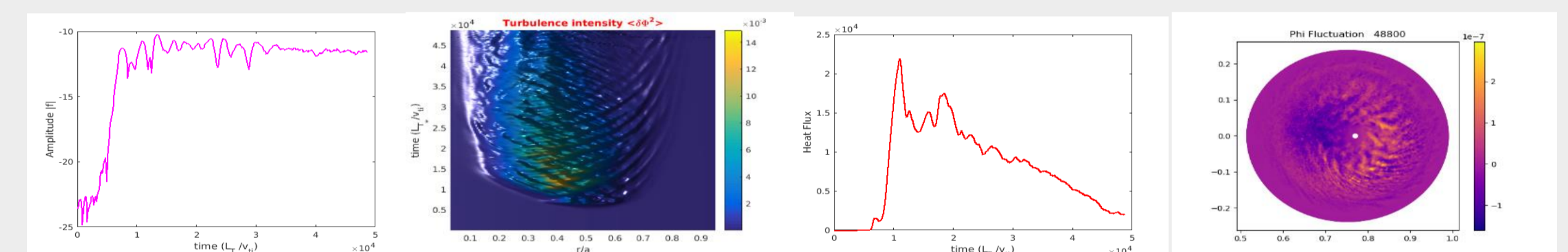


- ❖ In Fig. 5, upper and bottom panel shows real frequency and growth rate from GLOGYSTO and GTS codes for the value $R/L_n = 10$.
- ❖ From Fig. 5 we can see that, it exhibits two peaks in contrast to the single peak around $k_\theta \rho_i = 0.4$ generally observed in the linear analysis of the standard ITG modes using GLOGYSTO code. The second peak appears around $k_\theta \rho_i = 1.3$ and is characteristic of the SWITG mode
- ❖ Fig. 6 shows mode structure (from GLOGYSTO) for toroidal mode numbers $n=35$ and $n=110$.
- ❖ For comparison with a situation without SWITG, we have looked at $R/L_n = 5$ keeping $\eta = L_n/L_T$ fixed. To ensure that indeed SWITG is suppressed, flux tube GENE is run for both cases and it indeed suggests that for $R/L_n = 5$, SWITGs contribution would be small as shown in Fig. 7.
- ❖ Since GTS simulation is much more expensive therefore few n scans are presented with GTS. The complete toroidal mode number scan for the GTS are still under process.
- ❖ Standard ITG single peak around $k_\theta \rho_i = 0.7$ using GTS can also be seen from Fig. 5. we also see that there are differences in growth rate and real frequency values between GLOGYSTO and GTS, finding an explanation of this differences are ongoing.

Non-linear simulation of shot# 29029 of ADITYA-U tokamak using GTS

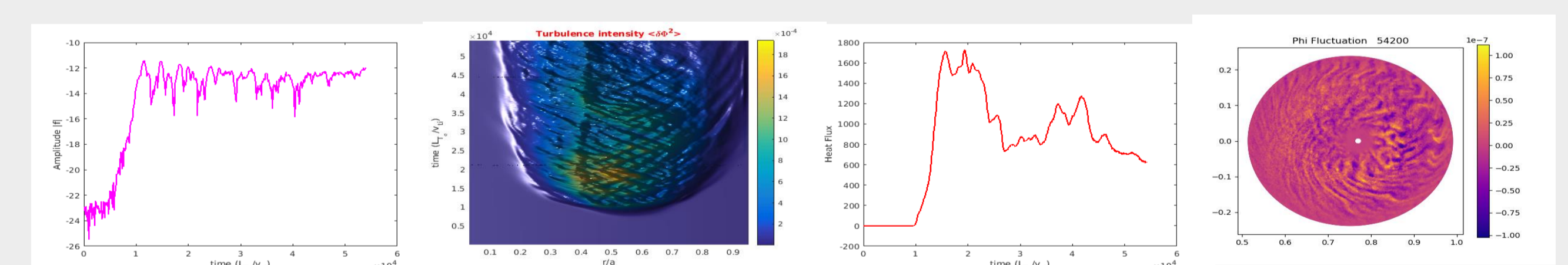
- Following the linear simulation, in this section we present nonlinear global simulations with GTS for $R/L_n = 10$ (experimental profiles with inherently multiscale ITGs in ADITYA-U) and $R/L_n = 5$ (to check how transport looks like if SWITG is suppressed) keeping η fixed.

1. $R/L_n = 10$ case: SWITG dominant case

Fig. 8 a) Mode amplitude, b) turbulence intensity, c) heat flux and d) mode structure plots for $R/L_n = 10$.

- Fig. 8 shows the results from the nonlinear simulation from GTS for higher temperature and density gradient cases.
- Fig. 8a presents the mode amplitude as a function of time. It is clear that after the initial linear phase the mode amplitude tends to saturate from time $t \sim 1.0 \times 10^4 v_{ti}/L_T$.
- The second panel, that is, Fig. 8b shows the spatiotemporal behaviour of the turbulence intensity. The mode intensity peaks at time $t \sim 1.0 \times 10^4 v_{ti}/L_T$ and around $r/a = 0.4-0.5$.
- The turbulence exists and spreads over a wide radial domain approximately from $r/a = 0.3$ to $r/a = 0.65$.
- The time-averaged heat flux in the steady state is around 2.0×10^3 in the normalised unit as shown in Fig. 8c.
- The right-most panel shows the structures of Φ in the nonlinear phase on the poloidal plane. The snapshot is taken at $t \sim 48800 v_{ti}/L_T$.
- The effect of zonal flow shearing of the potential is apparent from the snapshot. The zonal flow tears the global structures which regulates the turbulence. Also, the nonlinear turbulence spreading is evident from the figure.

2. $R/L_n = 5$ case: Conventional ITG dominant case

Fig. 9 a) Mode amplitude, b) turbulence intensity, c) heat flux and d) mode structure plots for $R/L_n = 5$

- Again, the mode amplitude is shown in Fig.9a. The mode amplitude increases and starts to saturate beyond $t \sim 1.0 \times 10^4 v_{ti}/L_T$. It is clear that compared to Fig.8a the mode amplitude increases slowly due to the reduced strength of the gradients. The spatio-temporal evolution of turbulence intensity is presented in Fig.9b which peaks between $r/a = 0.5$ and 0.6 and time around $t \sim 1.5 \times 10^4 v_{ti}/L_T$.
- The time averaged heat flux in the steady state is around $t \sim 6.0 \times 10^2$ in normalised unit as see in Fig. 9c. The steady state flux is quite smaller in the present case for $R/L_n = 5$ compared to the earlier case where $R/L_n = 10$ for fixed $\eta = L_n/L_T$. The snapshot of turbulent Φ on the poloidal plane is shown in Fig.9d for $t = 54200$. The effect of zonal flow is clearly visible from the figure.
- Note that these are preliminary results. More simulations regarding convergence with respect to spatial resolution, time step, particle/cell, etc., are going on.

Summary and Conclusion

- GTS code is first benchmarked for ion temperature gradient modes with a simplified adiabatic response for the electron dynamics for the CBC.
- Linear simulation studies of the conventional and shorter scale ion temperature gradient mode (SWITG) for experimental profiles and parameters of shot# 29029 of ADITYA-U tokamak are carried out using the global codes GLOGYSTO and GTS.
- Flux-tube GENE results in linear regime for comparison with GLOGYSTO and GTS results.
- There are differences in growth rate and real frequency values between GLOGYSTO and GTS, finding an explanation of this differences are ongoing.
- From the linear results, we observed two peaks in contrast to the single peak generally observed in the linear analysis of the standard ITG modes. The second peak appears around $k_\theta \rho_i = 1.3$ and is characteristic of the SWITG mode. It is found using linear stability analysis that the SWITGs are suppressed for low values of R/L_n .
- Nonlinear global simulations using GTS for ADITYA-U tokamak are also performed for $R/L_n = 10$ (experimental profiles with inherently multiscale ITGs in ADITYA-U) and $R/L_n = 5$ (to check how transport looks like if SWITG is suppressed) keeping η fixed.

References

- [1] Smolyakov A et al., Phys. Rev. Lett. 89, 125005 (2002).
- [2] Chowdhury J et al., Phys. Plasmas 18, 112510 (2011).
- [3] Chowdhury J et al., Phys. Plasmas 19, 042503 (2012).
- [4] F. Wagner et al., Phys. Rev. Lett. 53 (1984).
- [5] Gao Z et al., Phys. Plasmas 10, 2831 (2003).
- [6] R.L. Tanna et al., Nuclear Fusion 59, (2019).
- [7] W. X. Wang et al., Phys. Plasmas 13, 092505 (2006).
- [8] S. Brunner and J. Vaclavik, Phys. Plasmas 5, (1998).
- [9] F. Jenko et al., Phys. Plasmas 7, 1904 (2000).
- [10] T. Görler et al., Journal of Computational Physics 230 (2011) 7053–7071.
- [11] A.M. Dimits et al., Physics of Plasmas 7, 969 (2000).

ACKNOWLEDGMENTS:

This work is performed in IPR's HPC facility ANTYA at the Institute for Plasma Research, Gandhinagar, INDIA.